

1 **Potential of MALDI-TOF MS biotyping to detect deltamethrin resistance in the dengue vector *Aedes aegypti*.**

2

3 Lionel Almeras<sup>1,2,3\*</sup>, Monique Melo Costa<sup>1,2,3</sup>, Rémy Amalvict<sup>1,2,3,4</sup>, Joseph Guilliet<sup>5</sup>, Isabelle Dusfour<sup>6</sup>, Jean-Philippe  
4 David<sup>5</sup>, Vincent Corbel<sup>7,8</sup>.

5

6 <sup>1</sup>Unité Parasitologie et Entomologie, Département Microbiologie et Maladies Infectieuses, Institut de Recherche  
7 Biomédicale des Armées, 13005 Marseille, France.

8 <sup>2</sup>Aix Marseille Univ, IRD, AP-HM, SSA, VITROME, 13005 Marseille, France.

9 <sup>3</sup>IHU-Méditerranée Infection, 13005 Marseille, France.

10 <sup>4</sup>Centre National de Référence du Paludisme, 13005 Marseille, France.

11 <sup>5</sup> Laboratoire d'Ecologie Alpine, UMR UGA-USMB-CNRS 5553, Université Grenoble Alpes, 38041 Grenoble Cedex 9,  
12 France.

13 <sup>6</sup>Vectopôle Amazonien Emile Abonnenc, Unité de contrôle et adaptation des vecteurs, Institut Pasteur de la Guyane,  
14 Cayenne cedex, France.

15 <sup>7</sup>MIVEGEC, IRD, CNRS, University of Montpellier, Montpellier, France.

16 <sup>8</sup>Fundacao Oswaldo Cruz (FIOCRUZ), Instituto Oswaldo Cruz (IOC), Laboratório de Fisiologia e Controle de Artrópodes  
17 Vetores (Laficave). Avenida Brasil, 4365 Manguinhos, Rio de Janeiro – RJ, CEP: 21040-360, Brazil

18

19

20 **\*Corresponding author:** Dr. Lionel ALMERAS. Unité de Parasitologie et Entomologie (IRBA), Institut Hospitalo-  
21 Universitaire Méditerranée Infection, 19-21 Boulevard Jean Moulin 13385 Marseille cedex 05, France. Phone: 33 (0) 4  
22 91 32 43 75. Fax: 33 (0) 4 91 83 03 90. E-mail address: [almeras.lionel@gmail.com](mailto:almeras.lionel@gmail.com).

23 **Authors' emails:** LA : [almeras.lionel@gmail.com](mailto:almeras.lionel@gmail.com) ; MMC: [mcosta.monique@gmail.com](mailto:mcosta.monique@gmail.com); RA : [remy\\_alt@yahoo.fr](mailto:remy_alt@yahoo.fr);  
24 JG : [joseph.guilliet@gmail.com](mailto:joseph.guilliet@gmail.com) ; JPD: [jean-philippe.david@univ-grenoble-alpes.fr](mailto:jean-philippe.david@univ-grenoble-alpes.fr); VC: [vincent.corbel@ird.fr](mailto:vincent.corbel@ird.fr).

25

26 **Running title: MS detection of *Aedes aegypti* deltamethrin resistance**

27

28 **Abstract**

29 Insecticide resistance in mosquitoes is spreading worldwide and represents a growing threat to vector control. Insecticide  
30 resistance is caused by different mechanisms including higher metabolic detoxication, target-site modification, reduced  
31 penetration and behavioral changes that are not easily detectable with simple diagnostic methods. Indeed, most molecular  
32 resistance diagnostic tools are costly and labor intensive and then difficult to use for routine monitoring of insecticide  
33 resistance. The present study aims to determine whether mosquito susceptibility status against the pyrethroid insecticides  
34 (mostly used for mosquito control) could be established by the protein signatures of legs and/or thoraxes submitted to  
35 MALDI-TOF Mass Spectrometry (MS). The quality of MS spectra for both body parts was controlled to avoid any bias  
36 due to unconformity protein profiling. The comparison of MS profiles from three inbreds *Ae. aegypti* lines from French  
37 Guiana (IRF, IR03, IR13), with distinct deltamethrin resistance genotype / phenotype and the susceptible reference  
38 laboratory line BORA (French Polynesia), showed different protein signatures. On both body parts, the analysis of whole  
39 protein profiles revealed a singularity of BORA line compared to the three inbreeding lines from French Guiana origin,  
40 suggesting that the first criteria of differentiation is the geographical origin and/or the breeding history rather than the  
41 insecticide susceptibility profile. However, a deeper analysis of the protein profiles allowed to identify 10 and 11  
42 discriminating peaks from leg and thorax spectra, respectively. Among them, a specific peak around 4870 Da was detected  
43 in legs and thoraxes of pyrethroid resistant lines compared to the susceptible counterparts hence suggesting that MS  
44 profiling may be promising to rapidly distinguish resistant and susceptible phenotypes. Further work is needed to confirm  
45 the nature of this peak as a deltamethrin resistant marker and to validate the routine use of MS profiling to track insecticide  
46 resistance in *Ae. aegypti* field populations.

47

48 **Author Summary.**

49 The monitoring of mosquito insecticide resistance in local populations is essential to guide the choice of the vector control  
50 strategy. Current methods for resistance monitoring rely on biological, biochemical and molecular assays that all have  
51 their weakness. To circumvent these limitations, alternative methods have to be explored. In previous studies, MALDI-  
52 TOF MS profiling have proved its performance to classify mosquitoes at the species and sub-species levels. The present  
53 work aim was to assess whether MALDI-TOF MS profiling strategy could be useful for determination of mosquito  
54 susceptibility to the most used pyrethroid insecticide. In this way, four mosquito lines with distinct deltamethrin resistance  
55 genotype / phenotype were submitted to MS analysis. The accurate comparison of MS spectra showed different peak  
56 intensities between mosquitoes exhibiting different insecticide resistance profiles. Among discriminant peaks, one may  
57 be promising to detect insecticide-resistance mechanisms in public health mosquitoes. A better characterization of  
58 mosquito life traits will help countries to implement timely and locally adapted vector control interventions.

59

60 **Keywords:** *Aedes aegypti*; Deltamethrin; Insecticide resistance; MALDI-TOF MS; Innovative Diagnostic tool.

61 **Introduction**

62 *Aedes (Ae.) aegypti* (Diptera: Culicidae) is an urban mosquito species that can transmit viruses to humans causing  
63 infectious diseases, such as dengue, yellow fever, Zika, and chikungunya [1]. The geographic distribution of this pest is  
64 the widest ever recorded in history and it represents an increasing public health threat. The absence of specific antiviral  
65 treatments and the lack of vaccines or when available the low vaccination coverage underlined that the best protection  
66 method remains to avoid human exposure to *Ae. aegypti* bites [2]. Larval source management, community mobilization  
67 and chemical insecticides remain the first line of defense against this pest [3,4]. Unfortunately, the continuous use of  
68 public health pesticides for more than 40 years increased aversion of citizens to strategies based solely on insecticides  
69 because of their potential impacts on the environment and global health [4]. Furthermore, the use of the same insecticides  
70 in vector control for decades has selected mosquito resistances to all public health insecticides. Resistance in *Ae. aegypti*  
71 and *Ae. albopictus* is now present in at least 57 countries in South East Asia, Africa, the Americas and the Caribbean,  
72 where the burden of arboviral diseases is the highest [5]. Evidence of reduced susceptibility to insecticides has also been  
73 recently reported in invasive *Aedes* mosquitoes in Europe, especially from Italy, Greece and Spain [6,7], hence confirming  
74 that resistance is spreading rapidly across continents. In this context, there is a need for more adequate, scalable and  
75 affordable tools for tracking insecticide resistant mosquitoes in the field to prevent further spread.

76 Different mechanisms are known to confer resistance to chemical insecticides. One of the most widespread and known  
77 mechanisms is knockdown resistance (*kdr*) causing resistance to dichlorodiphenyltrichloroethane (DDT) and pyrethroids  
78 [8]. The mechanism is associated with point mutations affecting the gene encoding the voltage-gated sodium channel  
79 (VGSC), which is involved in the beginning and propagation of action potentials in the nervous system [8]. The  
80 mechanism was originally discovered in the housefly and then identified in a large number of arthropods including  
81 mosquitoes [9,10]. In *Ae. Aegypti*, several *kdr* mutations are known to confer resistance to pyrethroids and DDT including  
82 the V410L (a substitution of a valine to leucine at position 410), S989P, V1016I/G (i.e. a substitution of a valine to either  
83 isoleucine or glycine at position 1016) and F1534C (i.e. a substitution of a phenylalanine to cysteine at position 1534)  
84 mutations that were found in different regions of the world [11]. In addition, metabolic resistance through the over-  
85 expression of detoxifying enzymes belonging to Monooxygenases (P450s), Glutathione-S-Transferases (GSTs) and  
86 Carboxylesterases (CCEAs) can also confer high level of resistance to various classes of insecticides including  
87 pyrethroids [12,13]. Recent studies showed that additional mechanisms such as reduced insecticide penetration due to  
88 change in the thickness and/or composition of the cuticle [14,15] confer the insect the capacity to resist to multiple classes  
89 of insecticides.

90 Current methods for resistance monitoring rely on biological, biochemical and molecular assays that all have technical  
91 and/or operational constraints (e.g. lack of sensitivity or specificity, cost, low throughput). The strength and weakness of  
92 each method were previously reported by Dusfour et al [16]. Developing novel affordable and accurate strategies to detect

93 resistant mosquitoes at high-throughput would facilitate the implementation of timely and locally adapted insecticide  
94 resistance management strategies.

95 Recently, an innovative method based on the analysis of protein profiles obtained by Matrix-Assisted Laser  
96 Desorption/Ionization time-of-flight mass spectrometry (MALDI-TOF MS) profiling, was applied to arthropod  
97 identification [17,18]. Since 2013, we conducted pioneering studies, applying successfully this approach to the  
98 identification of several arthropod family such as mosquitoes, ticks, fleas or culicoides [19–22] as well as to the  
99 identification of blood source of engorged mosquitoes [23]. The principle of the classification is based on matching of  
100 query MS profiles with a MS reference spectra database (RSDB). The correct classification requires however that MS  
101 spectra are intra-species reproducible and inter-species specific. As for most phenotypic approaches, MS protein profiles  
102 could vary according to body part, developmental stages or sample preparation mode [24]. Then, to compare and to share  
103 MS results, a standardization of the protocols were previously established for mosquitoes [25,26]. We also showed that  
104 the independent submission of legs and thorax from the same specimen to MALDI-TOF MS [27] can improve the  
105 identification rate and confidence level, that may be decisive for discriminating similar phenotypes, such as cryptic species  
106 [26,28].

107 In this context, the aim of the present work was to determine whether resistance to the pyrethroid deltamethrin, could be  
108 detected in *Ae. aegypti* by analyzing the protein signatures of legs and/or thoraxes resulting from MALDI-TOF MS. In  
109 this way, MS profiles from four *Ae. aegypti* colonies, including one susceptible reference laboratory line from French  
110 Polynesia and three inbreeding lines from French Guiana showing distinct resistance phenotypes to deltamethrin were  
111 compared.

112

## 113 **Material and methods**

### 114 *Mosquito laboratory breeding*

115 Four *Ae. aegypti* colonies, including the susceptible reference laboratory line Bora-Bora (BORA) and three isofemale  
116 lines from French Guiana with distinct deltamethrin resistance phenotypes were used. The first two *Ae. aegypti* lines,  
117 (IR13 and IR03 lines) were obtained from gravid females collected in the Ile Royale, an island off the coast of Cayenne,  
118 by the Pasteur Institute of French Guiana [29]. According to WHO manual for monitoring insecticide resistance, the IR13  
119 line presented a slight tolerance to deltamethrin (mortality to discriminating concentration of deltamethrin  $\geq 90\%$ , but  
120 lower than 98%) and was considered as susceptible, whereas the IR03 line was considered as resistant to deltamethrin  
121 (mortality  $<90\%$  to the discriminating concentration of deltamethrin) [30]. Previous study supported the absence of the  
122 V410L, S989P and V1016I/G *kdr* mutations in both IR03 and IR13 lines. However, both IR13 and IR03 lines initially  
123 carried the F1534C mutation at moderate frequency [29]. Another resistant line deprived from the F1534C *kdr* mutation  
124 (IRF) was created by internal crossing of the IR03 line. Despite the absence of the F1534C mutation, the IRF line remained

125 resistant to deltamethrin [31], supporting the importance of metabolic resistance alleles in both resistant lines as  
126 previously shown [12,29,32,33]. All mosquito lines were reared using standard methods [27]. For eggs production, blood-  
127 meals were given through a Parafilm-membrane (hemotek membrane feeding systems, Discovery Workshops, UK) as  
128 previously described [24]. Larvae were reared until the pupal stage in trays containing 1liter distilled water supplemented  
129 with fish food (TetraMinBaby, Tetra GmbH, Herrenteich, Germany). Pupae were daily collected and transferred to  
130 mosquito cages (Bug Dorm 1, Bioquip products). For mass spectrometry (MS) analysis, pupae female, distinguished by  
131 sexual dimorphism, were transferred to mosquito cages. Twenty virgin, non-blood fed, 3 days-old females per line were  
132 collected and frozen at -20°C until MS analysis.

133

134 *Mosquito dissection*

135 Legs and thoraxes of each mosquito were processed as previously described [34]. Briefly, *Aedes* specimens were  
136 individually dissected, under a binocular loupe, with a sterile surgical blade. For each specimen, legs and thorax (without  
137 wings) were transferred in distinct 1.5 mL Eppendorf tubes for MALDI-TOF MS analysis. The remaining body parts  
138 (abdomens, wings and heads) were preserved for molecular analyses.

139

140 *Knockdown resistance (kdr) genotyping*

141 Genomic DNA was extracted individually from the remaining body parts (abdomen, wings and head) of 20 individual  
142 adult specimens per line using the QIAamp DNA tissue extraction kit (Qiagen, Hilden, Germany), according to the  
143 manufacturer's instructions. The kdr genotyping of V410L (a substitution of a valine to leucine at position 410), V1016I/G  
144 (i.e. a substitution of a valine to either isoleucine or glycine at position 1016) and F1534C (i.e. a substitution of a  
145 phenylalanine to cysteine at position 1534) were conducted by standard PCR (Table S1) followed by sequencing as  
146 previously described [35].

147

148 *Sample homogenization and MALDI-TOF MS analysis*

149 Each body part (legs and thorax) was homogenized individually for 3 x 1 minute at 30 Hertz using TissueLyser (Qiagen)  
150 and glass beads (#11079110, BioSpec Products, Bartlesville, OK, US) in a homogenization buffer composed of a mix  
151 (50/50) of 70% (v/v) formic acid (Sigma) and 50% (v/v) acetonitrile (Fluka, Buchs, Switzerland) according to the  
152 standardized automated setting as described previously [27]. After sample homogenization, a quick spin centrifugation at  
153 200 g for 1 min was then performed and 1 µL of the supernatant of each sample was spotted on the MALDI-TOF steel  
154 target plate in duplicate (Bruker Daltonics, Wissembourg, France). After air-drying, 1 µL of matrix solution composed  
155 of saturated  $\alpha$ -cyano-4-hydroxycinnamic acid (Sigma, Lyon, France), 50% (v/v) acetonitrile, 2.5% (v/v) trifluoroacetic  
156 acid (Aldrich, Dorset, UK) and HPLC-grade water was added. To control matrix quality (i.e. absence of MS peaks due

157 to matrix buffer impurities) and MALDI-TOF apparatus performance, matrix solution was loaded in duplicate onto each  
158 MALDI-TOF plate alone. Protein mass profiles were obtained using a Microflex LT MALDI-TOF Mass Spectrometer  
159 (Bruker Daltonics, Germany), with detection in the linear positive-ion mode at a laser frequency of 50 Hz within a mass  
160 range of 2-20 kDa. The setting parameters of the MALDI-TOF MS apparatus were identical to those previously used  
161 [36].

162

163 *MS spectra analysis*

164 MS spectra profiles were firstly controlled visually with flexAnalysis v3.3 software (Bruker Daltonics). MS spectra were  
165 then exported to ClinProTools v2.2 and MALDI-Biotyper v3.0. (Bruker Daltonics) for data processing (smoothing,  
166 baseline subtraction, peak picking). MS spectra reproducibility was assessed by the comparison of the average spectral  
167 profiles (MSP, Main Spectrum Profile) obtained from the two spots of each specimen from legs and thorax according to  
168 *Aedes* lines with MALDI-Biotyper v3.0 software (Bruker Daltonics). MS spectra reproducibility and specificity were  
169 achieved using cluster analyses and Composite Correlation Index (CCI) tool. Cluster analyses (MSP dendrogram) were  
170 performed based on comparison of the MSP given by MALDI-Biotyper v3.0. software and clustered according to protein  
171 mass profile (i.e. their mass signals and intensities). The CCI tool from MALDI-Biotyper v3.0. software was also used,  
172 to assess the spectral variations within and between each sample group, as previously described [20,27]. CCI matrix was  
173 calculated using MALDI-Biotyper v3.0. software with default settings (mass range 3.0-12.0 kDa; resolution 4; 8 intervals;  
174 auto-correction off). Higher correlation values (expressed by mean  $\pm$  standard deviation – SD) reflecting higher  
175 reproducibility for the MS spectra, were used to estimate MS spectra distance between lines. To visualize MS spectra  
176 distribution according to insecticide susceptibility, a principal component analysis (PCA) from ClinProTools v2.2  
177 software was used with the default settings.

178 The spectra were then analysed with the genetic algorithm (GA) model, which displayed a list of discriminating peaks  
179 between the two insecticide susceptible lines (BORA and IR13) and the two resistant lines (IR03 and IFR). A manual  
180 inspection and validation of the selected peaks by the operator gave a recognition capability (RC) value together with the  
181 highest cross-validation (CV) value. The presence or absence of all discriminating peak masses generated by the GA  
182 model was controlled by comparing the average spectra from line per body-part.

183

184 *Database creation and blind tests*

185 The reference MS spectra were created using spectra from two specimens per line and per body parts (legs and thorax)  
186 using MALDI-Biotyper software v3.0. (Bruker Daltonics). MS spectra were created with an unbiased algorithm using  
187 information on the peak position, intensity and frequency. The remaining MS spectra per line and body part were queried  
188 against these reference MS spectra and a classification as deltamethrin-resistant or –susceptible was done according to

189 the result of spectral matching with DB. The reliability of sample classification was determined using the Log Score  
190 Values (LSVs) given by the MALDI-Biotyper software v.3.0, corresponding to a matched degree of mass spectra between  
191 the query and the reference spectra from the DB. LSVs ranging from 0 to 3 were obtained for each spectrum of the  
192 samples tested. According to previous studies [28,37], LSVs greater than 1.8 were considered reliable for species  
193 identification. For evaluating its performance, the sensitivity, the specificity, the accuracy and the Cohen's  $\kappa$  coefficient,  
194 corresponding to the degree of agreement [38], were calculated.

195

196 *Statistical analyses*

197 After verifying that the LSVs in each line did not follow a Gaussian distribution (Shapiro-Wilk test), Wilcoxon matched-  
198 pairs signed-rank tests were computed when appropriate using GraphPad Prism v7.00 (GraphPad Software, La Jolla  
199 California USA.). Frequencies were compared by the Chi-square test. All differences were considered significant at  $p <$   
200 0.05. For detection of discriminant MS peaks, statistical tests from ClinProTools v2.2 software, including t-test  
201 (ANOVA), the Wilcoxon or Kruskal-Wallis (W/KW) test and the Anderson-Darling (AD) test were applied, to short  
202 peaks among profiles. To consider a peak as discriminant, it should obtain a significant  $p$ -value ( $<0.05$ ) in the AD test  
203 but also in the W/KW or ANOVA tests [39]. Among these discriminant MS peaks were selected those which presented  
204 a fold change upper than 1.3-fold between susceptible and resistant lines [40].

205

206 **Results**

207 *Low MS spectra diversity between Ae. aegypti lines.*

208 Legs and thoraxes from 20 specimens per line (BORA, IR13, IR03 and IRF) were submitted independently to MALDI-  
209 TOF MS analysis (Figure 1). At the exception of the legs from one specimen from the IR03 line, MS profiles of high  
210 intensity (>2000 a.u.) were obtained for all samples from both body parts. To control MS spectra “quality”, they were  
211 queried against our MS spectra database (DB) which includes reference MS spectra of legs and thoraxes from 16 distinct  
212 mosquito species [27,28] and notably *Ae. aegypti*. One hundred percent of the legs and thoraxes MS spectra matched with  
213 reference MS spectra from *Ae. aegypti* with respective body parts. Respectively, 97.5% (78/80) and 100% (80/80) of the  
214 MS spectra from legs and thoraxes reached the threshold LSV of 1.8 considered as a successful identification (Figure 2A  
215 and 2B) [21,25]. It is interesting to note that LSVs from thoraxes were significantly higher than those obtained for legs  
216 (Wilcoxon test,  $p < 0.0001$ ). More than 98% (79/80) of the thoraxes presented a LSV upper than 2.0 whereas only 71.25%  
217 (57/80) of the MS spectra from legs reached this last threshold.

218 To assess MS spectra reproducibility according to each *Ae. aegypti* line, CCI matrix, MSP dendrogram and PCA were  
219 performed. The low CCI obtained for the comparisons of paired MS spectra between thoraxes and legs (mean  $\pm$  SD: 0.31  
220  $\pm$  0.11) sustained the specificity of each body-part protein profiles. As expected, higher CCI were obtained for specimens  
221 from the same line than between lines for each body part, excepted for IR03 legs (mean CCI $\pm$ SD = 0.61 $\pm$ 0.20, Figure  
222 2C). This lower CCI value was attributed to the lower quality of MS spectra from one sample of the IR03 line. Moreover,  
223 values from thorax CCIs were more elevated than those of legs supporting that MS profiles from thoraxes were more  
224 reproducible. Interestingly, higher thorax CCIs were obtained between the two resistant lines (IR03 and IRF) and the  
225 IR13 susceptible line (mean  $\pm$  SD: 0.93  $\pm$  0.10), compared to the laboratory susceptible line (BORA) (mean  $\pm$  SD: 0.77  
226  $\pm$  0.13). Similarly, the reproducibility of leg MS profiles was higher between lines originating from French Guiana.

227 To assess the reproducibility and specificity of the MS spectra from legs and thoraxes according to their deltamethrin  
228 resistance phenotype, a cluster analysis was performed. Two specimens per line were used for building a MSP  
229 dendrogram (Figure 2D). Legs and thoraxes clustered in distinct branches confirming the specificity of the MS spectra  
230 per body part. However, no gathering of the spectra was noticed according to the resistance status or line, excepted for  
231 BORA using the thoraxes. The PCAs performed per body part with spectra from all samples showed two clusters. One  
232 cluster encompassed the three lines from French Guiana (IR03, IR13 and IRF) and another one included the BORA line  
233 for spectra from thoraxes (Figure 2E) and legs (Figure 2F). These results highlighted that overall comparisons of MS  
234 profiles did not allow to clearly distinguish specimens according to their deltamethrin resistance status whatever the body-  
235 part tested.

236

237 *Identification of discriminant MS peaks between deltamethrin-resistant and -susceptible lines*

238 To assess whether it was possible to identify discriminating MS peaks according to the deltamethrin resistance status, the  
239 MS spectra from the 20 specimens per line were analyzed for each body part (leg and thorax), using ClinProTools  
240 software. Then, the average spectrum from the insecticide-resistant lines (IR03 and IRF) were compared to the susceptible  
241 lines (BORA and IR13). A total of 99 and 118 peaks were detected in the average spectra of legs and thoraxes,  
242 respectively. MS peaks were considered as discriminant if they have a fold change upper than 1.3-fold in either direction  
243 between the two groups and if these variations were considered as statistically significant according to criteria defined  
244 previously (see material and methods). After verification of the peak report, 10 and 11 MS peaks from legs and thoraxes  
245 respectively (Tables 1 and 2) were considered of significant different intensity between the two groups. To assess whether  
246 these MS peaks could be discriminatory among these groups, they were included in the genetic algorithm (GA) model  
247 from ClinProTools 2.2 software. The combination of the presence/absence of these MS peaks from each body part lead  
248 to high RC and CV values for legs (90.0% and 98.1% respectively) and also for thoraxes (92.5% and 97.5%, respectively).  
249 Interestingly, one potential discriminant MS peak was shared between the two body parts with a m/z of about 4870 Da,  
250 corresponding to peak #16 in legs (Figure 3A, 3B and 3C) and peak #29 in thorax (Figure 3D, 3E and 3F). This 4870 Da  
251 peak was of greater intensity in the deltamethrin resistant lines than in the two susceptible lines for both body parts (Tables  
252 1 and 2). Interestingly, this peak was among the MS peak presenting the higher fold change (>2.8 fold) between resistant  
253 and susceptible-lines for both body parts (Tables 1 and 2). Submitting this single peak to the GA model lead to RC and  
254 CV values of 78.2% and 85.5%, respectively for legs and 79.8% and 85.6%, respectively for thoraxes. The detection of  
255 this peak in the IR13 susceptible line though at a lower intensity confirmed that no single peak was found exclusive of  
256 resistant-group species but that the discrimination was more attributed to intensity variations.  
257

258 **Table 1.** List of the discriminant MS peaks from legs between deltamethrin-resistant (IR03 and IRF) and –susceptible  
259 (BORA and IR13) *Ae. aegypti* lines.

| Peak number | Mass (Da)           | PTTA       | PW/KW      | PAD        | Average peak intensity<br>(mean $\pm$ SD in a.u.) |                 | Fold change |
|-------------|---------------------|------------|------------|------------|---|-----------------|-------------|
|             |                     |            |            |            | R   | S               |             |
| 16          | 4871.1 <sup>#</sup> | < 0.000001 | 0          | < 0.000001 | 11.1 $\pm$ 7                                      | 3.59 $\pm$ 1.94 | 3.09        |
| 22          | 5387.5              | 0.00517    | 0.0132     | < 0.000001 | 6.2 $\pm$ 3.24                                    | 4.76 $\pm$ 2.2  | 1.30        |
| 41          | 7019.9              | < 0.000001 | < 0.000001 | < 0.000001 | 2.97 $\pm$ 1.05                                   | 1.94 $\pm$ 0.57 | 1.53        |
| 59          | 9072.5              | 0.000364   | 0.000132   | < 0.000001 | 5.51 $\pm$ 2.28                                   | 4.09 $\pm$ 2.1  | 1.35        |
| 64          | 9965.0              | 0.0000328  | 0.0000129  | 6.36E-06   | 3.09 $\pm$ 0.98                                   | 2.37 $\pm$ 0.89 | 1.30        |
| 70          | 10776.2             | 0.000345   | 0.00129    | < 0.000001 | 6.32 $\pm$ 4.17                                   | 3.99 $\pm$ 2.82 | 1.58        |
| 83          | 12242.5             | < 0.000001 | < 0.000001 | 0.000151   | 2.11 $\pm$ 0.58                                   | 1.53 $\pm$ 0.36 | 1.38        |
| 93          | 14036.2             | < 0.000001 | 0          | < 0.000001 | 1.42 $\pm$ 0.36                                   | 0.97 $\pm$ 0.18 | 1.46        |
| 96          | 14851.6             | 0.0000565  | 0.0000882  | < 0.000001 | 2.54 $\pm$ 1.17                                   | 1.78 $\pm$ 0.86 | 1.43        |
| 99          | 18145.0             | 5.79E-06   | 1.08E-06   | < 0.000001 | 1.27 $\pm$ 0.44                                   | 0.94 $\pm$ 0.34 | 1.35        |

260 #MS peaks for which mass-to-charge ratio (m/z) were similar with thoraxes MS peak list (see Table 2). Da, Dalton;  
261 PTTA, p-value obtained by t-test; PW/KW, p-value obtained by Wilcoxon/Kruskal-Wallis test; PAD, p-value obtained  
262 by Anderson-Darling test; a.u., arbitrary unit; R, deltamethrin-resistant lines; S, deltamethrin-susceptible lines.  
263

264 **Table 2.** List of the discriminant MS peaks from thoraxes between deltamethrin-resistant (IR03 and IRF) and –susceptible  
265 (BORA and IR13) *Ae. aegypti* lines.

| Peak number | Mass (Da)           | PTTA       | PW/KW      | PAD        | Average peak intensity<br>(mean $\pm$ SD in a.u.) |                 | Fold change |
|-------------|---------------------|------------|------------|------------|---|-----------------|-------------|
|             |                     |            |            |            | R   | S               |             |
| 5           | 3026.9              | 0.000465   | 0.00208    | < 0.000001 | 1.96 $\pm$ 0.99                                   | 1.47 $\pm$ 0.49 | 1.33        |
| 16          | 4075.2              | 0.125      | 0.0112     | < 0.000001 | 6.73 $\pm$ 8.2                                    | 5.02 $\pm$ 2.38 | 1.34        |
| 19          | 4432.1              | 0.0415     | 0.0175     | < 0.000001 | 2.84 $\pm$ 2.03                                   | 2.15 $\pm$ 1.69 | 1.32        |
| 20          | 4446.3              | 0.0265     | 0.00243    | < 0.000001 | 3.01 $\pm$ 2.11                                   | 2.18 $\pm$ 2.03 | 1.38        |
| 24          | 4569.6              | 0.000179   | 0.0000745  | < 0.000001 | 4.37 $\pm$ 1.93                                   | 3.22 $\pm$ 1.5  | 1.36        |
| 29          | 4869.5 <sup>#</sup> | < 0.000001 | 0          | < 0.000001 | 6.19 $\pm$ 4.22                                   | 2.19 $\pm$ 0.89 | 2.83        |
| 74          | 9066.7              | < 0.000001 | < 0.000001 | < 0.000001 | 1.7 $\pm$ 0.32                                    | 4.18 $\pm$ 2.92 | 0.41        |
| 75          | 9095.5              | < 0.000001 | < 0.000001 | < 0.000001 | 3.81 $\pm$ 1.74                                   | 2.28 $\pm$ 0.86 | 1.67        |
| 76          | 9140.8              | 9.98E-06   | < 0.000001 | < 0.000001 | 5.86 $\pm$ 3.84                                   | 3.38 $\pm$ 2.0  | 1.73        |
| 110         | 13267.5             | 2.19E-06   | 5.25E-06   | < 0.000001 | 1.13 $\pm$ 0.32                                   | 1.56 $\pm$ 0.62 | 0.72        |
| 114         | 14030.0             | < 0.000001 | < 0.000001 | 0.000017   | 0.89 $\pm$ 0.21                                   | 0.66 $\pm$ 0.11 | 1.35        |

266 #MS peaks for which mass-to-charge ratio (m/z) were similar with legs MS peak list (see Table 1). Da. Dalton; PTTA,  
267 p-value obtained by t-test; PW/KW, p-value obtained by Wilcoxon/Kruskal-Wallis test; PAD, p-value obtained by  
268 Anderson-Darling test; a.u., arbitrary unit; R, deltamethrin-resistant lines; S, deltamethrin-susceptible lines.

269  
270  
271 *Assessment of blind test strategy to discriminate deltamethrin-resistant from -susceptible lines*

272 MS spectra from two specimens per line and per body part were selected for creation of reference MS spectra (Additional  
273 file 1). These MS spectra were selected in order that those from the deltamethrin-resistant lines (IR03 and IRF) possessed  
274 the most discriminant peak detected in both body parts at about 4870 m/z, whereas, this MS peak was absent from the  
275 two susceptible lines (BORA, IR13). The remaining MS spectra from legs (n=144, 18 samples per lines (x4) loaded in  
276 duplicate (x2)) and from thoraxes (n=144) were queried against these reference MS spectra. Overall, 98.9% (n=285/288)  
277 of the MS spectra queried against the database, obtained LSVs over 2.0, and all (100%) reached the threshold established  
278 for relevant identification (LSVs>1.8) (Additional Figure S1). The assessment of concordance of classification results  
279 (resistant or susceptible) between blind tests and lines revealed an agreement of 77.1% with a Cohen's  $\kappa$  coefficient of  
280 0.542 corresponding to a moderate agreement of the data for legs. Similarly, a moderate agreement (76.4% with a Cohen's  
281  $\kappa$  coefficient of 0.528) was obtained for thoraxes. The sensitivity and specificity of blind test strategy were, respectively,  
282 72.2% and 81.9% for legs and 72.2% and 80.6% for thoraxes using the four *Ae. aegypti* lines as reference (Table 3).

283

284 **Table 3.** Comparison of the classification of *Ae. aegypti* lines according to deltamethrin-susceptibility.

|                               | Legs                     |                             | Thoraxes                 |                             |
|-------------------------------|--------------------------|-----------------------------|--------------------------|-----------------------------|
|                               | Lines                    |                             | Lines                    |                             |
|                               | Resistant<br>(IR03, IRF) | Susceptible<br>(BORA, IR13) | Resistant<br>(IR03, IRF) | Susceptible<br>(BORA, IR13) |
| Blind tests*                  | R                        | 59                          | 20                       | 58                          |
|                               | S                        | 13                          | 52                       | 14                          |
| Total                         |                          | 72                          | 72                       | 72                          |
| Agreement (%)                 |                          | 77.1%                       |                          | 76.4%                       |
| Cohen's $\kappa$ <sup>#</sup> |                          | 0.542 (Moderate agreement)  |                          | 0.528 (Moderate agreement)  |
| Sensitivity (%)               |                          | 72.2 %                      |                          | 72.2%                       |
| Specificity (%)               |                          | 81.9%                       |                          | 80.6%                       |

285 \*Results of spectra classification queried against the reference MS spectra included in the DB. <sup>#</sup>Coefficient of agreement,  
286 the agreement level is indicated into brackets, as previously defined [38]. DB, database; MS, mass spectrometry;  
287 Resistant, deltamethrin-resistant lines; Susceptible, deltamethrin-susceptible lines.

288

289 *Potential association between the 4870 m/z MS peak and kdr mutations*

290 For each specimen tested in the present study, the V410L, V1016G/I, and F1534C kdr mutations were genotyped in an  
291 attempt to identify their potential association with the 4870 m/z MS resistance discriminating peak. These SNPs were  
292 selected because they are known to be strongly associated to pyrethroid resistance in *Ae. aegypti* [41–43]. Among the 20  
293 specimens tested for each line, genotyping failed for 5 individuals (i.e. one IR13, one IRF and three IR03). All genotyped  
294 specimens from BORA, IR13 and IRF lines were free of *kdr* mutations in all three sites of VGSC gene (i.e., genotype  
295 frequency of 100% for VV/VV/FF haplotype), while 65% of IR03 lines were heterozygotes (haplotype VV/VV/FC) and  
296 6% were homozygote resistant (haplotype VV/VV/CC) for the F1534C mutation (Table 4).

297 As the four lines were confirmed to be susceptible for the V410L and V1016G/I mutations, the potential association  
298 between the F1534C mutation and the 4870 m/z MS peak was investigated. The classification of the leg and thorax spectra  
299 according to genotypes (FF, FC or CC) did not show any association between F1534C genotypes and the abundance of  
300 4870 m/z MS peak (Additional Figure S2). Indeed, the 4870 m/z MS peak was detected in half of the individuals carrying  
301 the mutation, either in heterozygosis or homozygosis mutant (FC or CC), and in all susceptible genotypes (FF) for both  
302 body parts. Altogether, this indicates that the 4870 m/z MS discriminant MS peak is not related to the V410L, V1016G/I,  
303 and F1534C *kdr* mutations.

304

305 **Table 4.** Genotyping of V410L, V1016I and F1534C *kdr* mutations in the four lines of *Aedes aegypti*.

**Genotypes (410/1016/1534)**

| <i>Ae. aegypti</i> lines | VV/VV/FF  | VV/VV/FC  | VV/VV/CC | Others combinations |
|--------------------------|-----------|-----------|----------|---------------------|
| BORA                     | 20        | 0         | 0        | 0                   |
| IR13                     | 19        | 0         | 0        | 0                   |
| IR03                     | 5         | 11        | 1        | 0                   |
| IRF                      | 19        | 0         | 0        | 0                   |
| <b>Total</b>             | <b>63</b> | <b>11</b> | <b>1</b> | <b>0</b>            |

306

307

308 **Discussion**

309 The success of MALDI-TOF MS profiling for mosquito species identification [44,45], detection of parasitic agents  
310 [34,46] and/or for the determination of blood feeding origin of engorged specimens [23,47] led us to investigate the  
311 potential of this tool for the detection of insecticide resistance. Here we focused on deltamethrin, the most widely used  
312 pyrethroid insecticide for the control of the main arboviral vector, *Ae. aegypti*. To reduce the impact of the genetic and  
313 environmental conditions on the outcomes, we selected three mosquito lines collected in the same region (French Guiana)  
314 and having close genetic backgrounds, including one line being susceptible to deltamethrin (IR13) and two confirmed  
315 deltamethrin-resistant lines (IR03 and IRF) [29]. In addition, the susceptible laboratory line Bora-Bora (BORA) carrying  
316 no resistance allele was tested to generate reference MS profile.

317 Prior to research MS peak markers associated to insecticide resistance, a quality control of the MS spectra was carried  
318 out by evaluating the accuracy of sample identification against a home-made reference spectrum DB. For the first query,  
319 no MS spectra from the three French Guiana *Ae. aegypti* lines were included in the spectra DB as reference. Nevertheless,  
320 a correct and relevant identification ( $LSV \geq 1.8$ ) was obtained for 98.8% (158/160) of the samples. The matching of these  
321 query leg and thorax MS spectra with those of *Ae. aegypti* from the DB coming from the laboratory (i.e., BORA) or the  
322 field [45] underlined that the spectra were conserved among these *Ae. aegypti* specimens from distinct origins  
323 (reproducibility of spectra). The presence of reference spectra from specimens of the same species was then sufficient for  
324 correct and reliable identification of species identification, confirming the compliance of the MS spectra dataset from legs  
325 and thoraxes for next analyses [24,27].

326 The significant higher LSVs obtained for thoraxes compared to legs confirmed the better MS spectra reproducibility of  
327 the thoraxes for species identification, as recently demonstrated [26]. Nevertheless, for both body parts, comparisons of  
328 CCI, cluster analysis and PCAs indicated that MS spectra were more reproducible among strains coming from the same  
329 geographical origin (the three lines from French Guiana) than from BORA line, which is originating from French  
330 Polynesia and has been maintained in the laboratory for more than 30 years. Indeed, the MS spectra from the BORA line  
331 slightly differed from those of French Guiana (IR03, IR13 and IRF) for both body parts, legs and thoraxes. These data  
332 also suggest that MS profiles from isofemale lines are closer among them than between specimens presenting the same  
333 properties regarding the deltamethrin susceptibility phenotype. These results are concordant with previous works which  
334 already reported that MS spectra from specimens of the same species were more homogeneous if they have the same  
335 geographical origin [21,26]. Then, the higher MS spectra homology according to specimen geographical origin underlined  
336 that the classification of specimens according to their deltamethrin susceptibility could not be elucidated by the analysis  
337 of the whole MS spectra, as it is commonly done for arthropod species classification by MALDI-TOF MS biotyping [48].  
338 Then, we focused our work by looking at specific MS peaks that could distinguish specimens according to their  
339 deltamethrin susceptibility.

340 The comparison of the average spectrum intensity between the IR03 and IRF deltamethrin-resistant and the BORA and  
341 IR13 susceptible lines revealed multiple MS peaks with significant abundance variations for legs and thoraxes. These  
342 peaks allowed to classify correctly more than 90.0% of the specimens after applying a GA model on both body parts.  
343 These data underlined that less than a dozen of MS peaks per body part appeared sufficient to segregate both groups.  
344 Such imperfect classification is probably explained by the inter-individual variability exists in the lines tested and by  
345 other resistant markers (e.g. metabolic) which may be present in the mosquitoes originated from French Guiana lines  
346 [29].

347 In this kind of study, the difficulty is coming from the heterogeneity or spectra variation which occurred among specimens  
348 from the same species but coming from distinct origins. That's why the main factors that can create spectra noise were  
349 controlled by using *Ae. aegypti* lines having the same genetic background (i.e. isofemales lines) and coming from the  
350 same geographical region. Moreover, the laboratory rearing of the four mosquito lines in standardized breeding conditions  
351 participated also to reduce spectra variation due to environmental factors. A recent study demonstrated that the application  
352 of machine learning models to MS spectra from legs or thoraxes from anopheline mosquitoes could detect biomarkers  
353 associated to diverse life history traits such as, the population age, past blood feeding or plasmodium infectious status  
354 [49].

355 Among the discriminant MS peaks, one peak, at about 4870 m/z, was found significantly more intense (fold change upper  
356 than 2.8) in deltamethrin-resistant lines as compared to the susceptible one's. This peak was found in legs and thoraxes.  
357 The application of GA model to this peak allowed to classify mosquito specimens as deltamethrin-susceptible or  
358 deltamethrin-resistant with a concordance of about 80%. Although promising, we have no guarantee that this peak is  
359 systematically and functionally associated to deltamethrin resistance. First of all, no association was found between *kdr*  
360 alleles at position 1534 (at heterozygote or homozygote haplotypes) and the abundance of 4870 m/z MS peak. No mutant  
361 *kdr* alleles were found at 1016 and 410 sites in all isofemale lines from French Guiana as initially reported [29], then no  
362 genotype-phenotype association studies were performed. Our data suggest that the deltamethrin resistance phenotype of  
363 the IR03 and IRF lines is not majorly caused by *kdr* mutations but most probably by other metabolic resistance alleles as  
364 previously reported [32]. In this regard, it is possible that the abundance of the 4870 m/z MS peak in deltamethrin-resistant  
365 lines rather reflects a change in the expression of particular detoxifying enzymes involved in deltamethrin-resistance,  
366 such as P450s. This peptide could also result from an indirect effect and could have a priori no causal link with the  
367 insecticide resistance phenotype. Clearly, further work is needed to assess the protein nature and function associated with  
368 this 4870 m/z MS peak. One way to do this may involve further association studies using the IRF line deprived from *kdr*  
369 mutations together with cross-comparison of MS data with molecular data obtained from loci associated with resistance.  
370 The tracking of this particular MS peak in a larger collection of resistant and susceptible populations may also help us to  
371 validate this association of this MS peak with resistance.

372 Finally, the functional characterization of the 4870 m/z MS peak is a priority. The identification of the protein/peptide  
373 will however require additional MS apparatus [50]. For example, the protein/peptide could identify by peptide-sequencing  
374 using tandem mass-spectrometry approach [51] and validated by immune detection (eg, ELISA, WB, etc) [52]. Regardless  
375 the technique, the identification and incrimination of this peak in deltamethrin-resistance could open the door for the  
376 development of novel diagnostic assays to track pyrethroid resistance.

377

378 **Conclusions**

379 The MALDI-TOF MS profiling is an innovative approach which proved to be a rapid, affordable and efficient method  
380 for the identification of vector species, blood feeding source and some pathogen infection. This emerging entomological  
381 strategy may also be relevant for identifying others mosquito life traits of major importance, such as insecticide resistance.  
382 Although, the analysis of global MS profiles failed to distinct susceptible to resistant phenotypes in the inbreed females,  
383 an accurate comparison of spectra allowed to reveal potential peaks associated to deltamethrin-resistance. This pioneering  
384 study requires further complementary experimental works and collaborative research efforts, to consider the potential  
385 outputs for the mosquito surveillance. The characterization of key mosquito life traits with a unique approach will be  
386 revolutionary for vector biology and the prevention of mosquito-borne diseases outbreaks.

387 **List of abbreviations**

388 *Ae.*: *Aedes*; CCI: Composite Correlation Index; CV: cross-validation; DDT: dichlorodiphenyltrichloroethane; GA: genetic  
389 algorithm; IR: insecticide resistance; kdr: knockdown resistance; LSV: Log Score Value; MALDI-TOF MS: Matrix  
390 Assisted Laser Desorption/Ionization Time-of-Flight Mass Spectrometry; MSP: Main Spectra Projection; PCA: principal  
391 component analysis; RC: recognition capability; RSDB: reference spectra database; VGSC: voltage-gated sodium  
392 channel.

393

394 **Declarations**

395 **Ethics approval and consent to participate**

396 Not applicable.

397

398 **Consent for publication**

399 Not applicable.

400

401 **Availability of data and materials**

402 The datasets of MS reference spectra added to the MS DB in the current study are freely available and downloadable  
403 from the Additional file S1.

404

405 **Competing interests**

406 The authors declare that they have no competing interests.

407

408 **Funding Statement**

409 This work has been supported by the Délégation Générale pour l'Armement (DGA, MSProfileR project, Grant no PDH-  
410 2-NRBC-2-B-2201) and the WIN (Worldwide Insecticide resistance Network).

411

412 **Authors' contributions**

413 Conceived and designed the experiments: LA and VC. Performed the experiments: LA, RA and MMC. Analyzed the  
414 data: LA, RA, VC and JPD. Contributed reagents/materials/analysis tools: LA, RA, JG, ID and JPD. Drafted the paper:  
415 LA and VC. Revised critically the paper: all authors.

416

417 **Acknowledgments**

418 We thank the “Fondation Méditerranée Infection (FMI)” which offered personnel grant to MMC and the WIN (Worldwide

419 Insecticide resistance Network) which contributed in the travelling of the student between Brazil and France.

420

421 **References**

- 422 1. Chala B, Hamde F. Emerging and Re-emerging Vector-Borne Infectious Diseases and the Challenges for Control:  
423 A Review. *Front Public Health*. **2021**; 9:715759.
- 424 2. Fontaine A, Diouf I, Bakkali N, et al. Implication of haematophagous arthropod salivary proteins in host-vector  
425 interactions. *Parasit Vectors*. **2011**; 4:187.
- 426 3. Corbel V, Achee NL, Chandre F, et al. Tracking Insecticide Resistance in Mosquito Vectors of Arboviruses: The  
427 Worldwide Insecticide resistance Network (WIN). *PLoS Negl Trop Dis*. **2016**; 10(12):e0005054.
- 428 4. Roiz D, Wilson AL, Scott TW, et al. Integrated Aedes management for the control of Aedes-borne diseases. *PLoS*  
429 *Negl Trop Dis*. **2018**; 12(12):e0006845.
- 430 5. Moyes CL, Vontas J, Martins AJ, et al. Contemporary status of insecticide resistance in the major Aedes vectors  
431 of arboviruses infecting humans. *PLoS Negl Trop Dis*. **2017**; 11(7):e0005625.
- 432 6. Kasai S, Caputo B, Tsunoda T, et al. First detection of a Vssc allele V1016G conferring a high level of insecticide  
433 resistance in *Aedes albopictus* collected from Europe (Italy) and Asia (Vietnam), 2016: a new emerging threat to  
434 controlling arboviral diseases. *Euro Surveill Bull Eur Sur Mal Transm Eur Commun Dis Bull*. **2019**; 24(5).
- 435 7. Fotakis EA, Chaskopoulou A, Grigoraki L, et al. Analysis of population structure and insecticide resistance in  
436 mosquitoes of the genus *Culex*, *Anopheles* and *Aedes* from different environments of Greece with a history of  
437 mosquito borne disease transmission. *Acta Trop*. **2017**; 174:29–37.
- 438 8. Auteri M, La Russa F, Blanda V, Torina A. Insecticide Resistance Associated with kdr Mutations in *Aedes*  
439 *albopictus*: An Update on Worldwide Evidences. *BioMed Res Int*. **2018**; 2018:3098575.
- 440 9. Martinez-Torres D, Chandre F, Williamson MS, et al. Molecular characterization of pyrethroid knockdown  
441 resistance (kdr) in the major malaria vector *Anopheles gambiae* s.s. *Insect Mol Biol*. **1998**; 7(2):179–184.
- 442 10. Brengues C, Hawkes NJ, Chandre F, et al. Pyrethroid and DDT cross-resistance in *Aedes aegypti* is correlated with  
443 novel mutations in the voltage-gated sodium channel gene. *Med Vet Entomol*. **2003**; 17(1):87–94.
- 444 11. Silva JJ, Kouam CN, Scott JG. Levels of cross-resistance to pyrethroids conferred by the Vssc knockdown  
445 resistance allele 410L+1016I+1534C in *Aedes aegypti*. *PLoS Negl Trop Dis*. **2021**; 15(7):e0009549.
- 446 12. Cattel J, Faucon F, Le Péron B, et al. Combining genetic crosses and pool targeted DNA-seq for untangling genomic  
447 variations associated with resistance to multiple insecticides in the mosquito *Aedes aegypti*. *Evol Appl*. **2020**;  
448 13(2):303–317.
- 449 13. Cattel J, Haberkorn C, Laporte F, et al. A genomic amplification affecting a carboxylesterase gene cluster confers  
450 organophosphate resistance in the mosquito *Aedes aegypti*: From genomic characterization to high-throughput field  
451 detection. *Evol Appl*. **2021**; 14(4):1009–1022.
- 452 14. Balabanidou V, Grigoraki L, Vontas J. Insect cuticle: a critical determinant of insecticide resistance. *Curr Opin*  
453 *Insect Sci*. **2018**; 27:68–74.
- 454 15. Balabanidou V, Kefi M, Aivaliotis M, et al. Mosquitoes cloak their legs to resist insecticides. *Proc Biol Sci*. **2019**;  
455 286(1907):20191091.
- 456 16. Dusfour I, Vontas J, David J-P, et al. Management of insecticide resistance in the major Aedes vectors of  
457 arboviruses: Advances and challenges. *PLoS Negl Trop Dis*. **2019**; 13(10):e0007615.
- 458 17. Yssouf A, Almeras L, Raoult D, Parola P. Emerging tools for identification of arthropod vectors. *Future Microbiol*.  
459 **2016**; 11(4):549–566.
- 460 18. Sevestre J, Diarra AZ, Laroche M, Almeras L, Parola P. Matrix-assisted laser desorption/ionization time-of-flight  
461 mass spectrometry: an emerging tool for studying the vectors of human infectious diseases. *Future Microbiol*. **2021**;  
462 .
- 463 19. Sambou M, Aubadie-Ladrix M, Fenollar F, et al. Comparison of matrix-assisted laser desorption ionization-time

464 of flight mass spectrometry and molecular biology techniques for identification of Culicoides (Diptera:  
465 ceratopogonidae) biting midges in senegal. *J Clin Microbiol.* **2015**; 53(2):410–418.

466 20. Diarra AZ, Almeras L, Laroche M, et al. Molecular and MALDI-TOF identification of ticks and tick-associated  
467 bacteria in Mali. *PLoS Negl Trop Dis.* **2017**; 11(7):e0005762.

468 21. Yssouf A, Parola P, Lindström A, et al. Identification of European mosquito species by MALDI-TOF MS. *Parasitol*  
469 *Res.* **2014**; 113(6):2375–2378.

470 22. Yssouf A, Socolovschi C, Leulmi H, et al. Identification of flea species using MALDI-TOF/MS. *Comp Immunol*  
471 *Microbiol Infect Dis.* **2014**; 37(3):153–157.

472 23. Niare S, Berenger J-M, Dieme C, et al. Identification of blood meal sources in the main African malaria mosquito  
473 vector by MALDI-TOF MS. *Malar J.* **2016**; 15:87.

474 24. Dieme C, Yssouf A, Vega-Rúa A, et al. Accurate identification of Culicidae at aquatic developmental stages by  
475 MALDI-TOF MS profiling. *Parasit Vectors.* **2014**; 7:544.

476 25. Nebbak A, Willcox AC, Bitam I, Raoult D, Parola P, Almeras L. Standardization of sample homogenization for  
477 mosquito identification using an innovative proteomic tool based on protein profiling. *Proteomics.* **2016**,  
478 16(24):3148–3160.

479 26. Bamou R, Costa MM, Diarra AZ, Martins AJ, Parola P, Almeras L. Enhanced procedures for mosquito  
480 identification by MALDI-TOF MS. *Parasit Vectors.* **2022**; 15(1):240.

481 27. Vega-Rúa A, Pagès N, Fontaine A, et al. Improvement of mosquito identification by MALDI-TOF MS biotyping  
482 using protein signatures from two body parts. *Parasit Vectors.* **2018**; 11(1):574.

483 28. Briolant S, Costa MM, Nguyen C, et al. Identification of French Guiana anopheline mosquitoes by MALDI-TOF  
484 MS profiling using protein signatures from two body parts. *PloS One.* **2020**; 15(8):e0234098.

485 29. Epelboin Y, Wang L, Giai Gianetto Q, et al. CYP450 core involvement in multiple resistance strains of Aedes  
486 aegypti from French Guiana highlighted by proteomics, molecular and biochemical studies. *PloS One.* **2021**,  
487 16(1):e0243992.

488 30. World Health Organization. Manual for monitoring insecticide resistance in mosquito vectors and selecting  
489 appropriate interventions [Internet]. 2022. Available from:  
490 <https://www.who.int/publications/i/item/9789240051089>

491 31. Bacot, T, Haberkorn C, Guilliet J, et al. A large genomic duplication spanning multiple P450s contributes to  
492 pyrethroid resistance in the dengue mosquito Aedes aegypti [Internet]. Petit Pois Déridé; 2022. Available from:  
493 <https://ppd2022.sciencesconf.org/resource/page/id/1>

494 32. Faucon F, Dusfour I, Gaude T, et al. Identifying genomic changes associated with insecticide resistance in the  
495 dengue mosquito Aedes aegypti by deep targeted sequencing. *Genome Res.* **2015**; 25(9):1347–1359.

496 33. Faucon F, Gaude T, Dusfour I, et al. In the hunt for genomic markers of metabolic resistance to pyrethroids in the  
497 mosquito Aedes aegypti: An integrated next-generation sequencing approach. *PLoS Negl Trop Dis.* **2017**,  
498 11(4):e0005526.

499 34. Tahir D, Almeras L, Varloud M, Raoult D, Davoust B, Parola P. Assessment of MALDI-TOF mass spectrometry  
500 for filariae detection in Aedes aegypti mosquitoes. *PLoS Negl Trop Dis.* **2017**; 11(12):e0006093.

501 35. Murcia O, Henríquez B, Castro A, et al. Presence of the point mutations Val1016Gly in the voltage-gated sodium  
502 channel detected in a single mosquito from Panama. *Parasit Vectors.* **2019**; 12(1):62.

503 36. Lafri I, Almeras L, Bitam I, et al. Identification of Algerian Field-Caught Phlebotomine Sand Fly Vectors by  
504 MALDI-TOF MS. *PLoS Negl Trop Dis.* **2016**; 10(1):e0004351.

505 37. Costa MM, Guidez A, Briolant S, et al. Identification of Neotropical Culex Mosquitoes by MALDI-TOF MS  
506 Profiling. *Trop Med Infect Dis.* **2023**; 8(3):168.

507 38. Landis JR, Koch GG. The measurement of observer agreement for categorical data. *Biometrics*. **1977**; 33(1):159–174.

509 39. Rocca MF, Zintgraff JC, Dattero ME, et al. A combined approach of MALDI-TOF mass spectrometry and multivariate analysis as a potential tool for the detection of SARS-CoV-2 virus in nasopharyngeal swabs. *J Virol Methods*. **2020**; 286:113991.

512 40. Fraisier C, Camoin L, Lim SM, et al. Altered protein networks and cellular pathways in severe west nile disease in mice. *PloS One*. **2013**; 8(7):e68318.

514 41. Hernandez JR, Liu S, Fredregill CL, Pietrantonio PV. Impact of the V410L kdr mutation and co-occurring 515 genotypes at kdr sites 1016 and 1534 in the VGSC on the probability of survival of the mosquito *Aedes aegypti* 516 (L.) to Permanone in Harris County, TX, USA. *PLoS Negl Trop Dis*. **2023**; 17(1):e0011033.

517 42. Linss JGB, Brito LP, Garcia GA, et al. Distribution and dissemination of the Val1016Ile and Phe1534Cys Kdr 518 mutations in *Aedes aegypti* Brazilian natural populations. *Parasit Vectors*. **2014**; 7:25.

519 43. Marcombe S, Mathieu RB, Pocquet N, et al. Insecticide resistance in the dengue vector *Aedes aegypti* from 520 Martinique: distribution, mechanisms and relations with environmental factors. *PloS One*. **2012**; 7(2):e30989.

521 44. Müller P, Pflüger V, Wittwer M, et al. Identification of cryptic *Anopheles* mosquito species by molecular protein 522 profiling. *PloS One*. **2013**; 8(2):e57486.

523 45. Yssouf A, Socolovschi C, Flaudrops C, et al. Matrix-assisted laser desorption ionization--time of flight mass 524 spectrometry: an emerging tool for the rapid identification of mosquito vectors. *PloS One*. **2013**; 8(8):e72380.

525 46. Laroche M, Almeras L, Pecchi E, et al. MALDI-TOF MS as an innovative tool for detection of *Plasmodium* 526 parasites in *Anopheles* mosquitoes. *Malar J*. **2017**; 16(1):5.

527 47. Tandina F, Laroche M, Davoust B, K Doumbo O, Parola P. Blood meal identification in the cryptic species 528 *Anopheles gambiae* and *Anopheles coluzzii* using MALDI-TOF MS. *Parasite Paris Fr*. **2018**; 25:40.

529 48. Abdellahoum Z, Nebbak A, Lafri I, et al. Identification of Algerian field-caught mosquito vectors by MALDI-TOF 530 MS. *Vet Parasitol Reg Stud Rep*. **2022**; 31:100735.

531 49. Nabet C, Chaline A, Franetich J-F, et al. Prediction of malaria transmission drivers in *Anopheles* mosquitoes using 532 artificial intelligence coupled to MALDI-TOF mass spectrometry. *Sci Rep*. **2020**; 10(1):11379.

533 50. Guthals A, Bandeira N. Peptide identification by tandem mass spectrometry with alternate fragmentation modes. 534 *Mol Cell Proteomics MCP*. **2012**; 11(9):550–557.

535 51. Zhang X, Scalf M, Berggren TW, Westphall MS, Smith LM. Identification of mammalian cell lines using MALDI- 536 TOF and LC-ESI-MS/MS mass spectrometry. *J Am Soc Mass Spectrom*. **2006**; 17(4):490–499.

537 52. Lefranc D, Dubucquois S, Almeras L, et al. Molecular analysis of endogenous retrovirus HRES-1: identification of 538 frameshift mutations in region encoding putative 28-kDa autoantigen. *Biochem Biophys Res Commun*. **2001**; 539 283(2):437–444.

540

541

542

543

## Figure legends

544

**Figure 1. Comparison of MALDI-TOF MS spectra from legs (A) and thoraxes (B) of four *Aedes aegypti* lines.** Representative MS spectra of two *Ae. aegypti* specimens per line, susceptible (BORA (a, b) and IR13 (c, d)) or resistant (IR03 (e, f) and IRF (g, h)) to deltamethrin. a.u., arbitrary units; m/z, mass-to-charge ratio.

545

**Figure 2. Reproducibility and specificity of MALDI-TOF MS spectra from *Aedes aegypti* lines according to body part.** LSVs obtained following homemade MS reference database query with MS spectra of the four *Ae. aegypti* lines from legs (A) and thoraxes (B). Twenty specimens per line were tested. Horizontal dashed lines represent the threshold value for reliable identification (LSV>1.8). LSVs, log score values; a.u., arbitrary units. (C) The same 20 MS spectra per line and body part were analysed using the composite correlation index (CCI) tool. Levels of MS spectra reproducibility are indicated in red and blue revealing relatedness and incongruence between spectra, respectively. The values correspond to the mean coefficient correlation and respective standard deviations obtained for paired condition comparisons. CCI were expressed as mean  $\pm$  standard deviation. (D) MSP dendrogram of MALDI-TOF MS spectra from legs (red) and thoraxes (blue) of the four *Ae. aegypti* lines. Two specimens per lines and per body part are presented. The distance units correspond to the relative similarity of MS spectra. The dendrogram was created by Biotyper v3.0 software. Principal Component Analysis (PCA) dimensional image from thoraxes (E, n=20) and legs (F, n=20) MS spectra of the four lines. Red, green, blue and yellow dots correspond to BORA, IR13, IR03 and IRF *Ae. aegypti* lines, respectively.

546

**Figure 3. Variation of the MS peak at about 4870 m/z among the four *Ae. aegypti* lines according to their susceptibility to deltamethrin.** Overlay mean profile view of leg (A) and thorax (D) body parts according to *Ae. aegypti* lines. Line color code of each mosquito line is indicated in the top right part. Gel view of leg (B) and thorax (E) MS spectra from the 20 specimens per line. The two replicates loaded on the MS plate for each specimen per body part are presented. The discriminant MS peak (m/z: 4870 Da) is indicated by an asterisk (\*). Graphical representation of the intensity of the 4870 m/z MS peak from legs (C) and thoraxes (F) according to *Ae. aegypti* lines. Standard deviations of intensities are represented by vertical lines. A.U.: arbitrary units; m/z: mass to charge ratio; R: lines classified deltamethrin-resistant; S: lines classified deltamethrin-susceptible. The same color code was used for all the panels.

547

## Supporting information

548

**Additional Figure S1. LSVs following upgrading homemade reference database with MS spectra from legs (A) and thoraxes (B) of the four *Ae. aegypti* lines.** Eighteen specimens per line were tested. Horizontal dashed lines represent the threshold value for reliable identification (LSV>1.8). Red, green, blue and yellow dots correspond to BORA, IR13, IR03 and IRF *Ae. aegypti* lines, respectively. LSVs, log score values; a.u., arbitrary units.

549

**Additional Figure S2. Variation of the MS peak at about 4870 m/z among the IR03 *Ae. aegypti* line according to their 1534 *kdr* genotyping.** Overlay mean profile view of leg (A) and thorax (D) body parts according to 1534 genotype. Line color code of each genotype is indicated in the top right part. Gel view of leg (B) and thorax (E) MS spectra from the IR03 specimens per genotype. The two replicates loaded on the MS plate for each specimen per body part are presented. The discriminant MS peak (m/z: 4870 Da) is indicated by an asterisk (\*). Graphical representation of the intensity of the 4870 m/z MS peak from legs (C) and thoraxes (F) according to 1534 genotype of IR03 *Ae. aegypti* line. Standard deviations of intensities are represented by vertical lines. A.U.: arbitrary units; m/z: mass to charge ratio; Red: haplotype homozygotes without mutation (VV/VV/FF); Green: mutant haplotype heterozygotes (VV/VV/FC) and homozygotes (VV/VV/CC). The same color code was used for all the panels.

550

**Additional file 1. Raw leg and thorax MS spectra from the four *Ae. aegypti* lines included in the MS reference database.** MS spectra were obtained using Microflex LT MALDI-TOF Mass Spectrometer (Bruker Daltonics). Details of each sample were listed of the excel file named “REF\_MS\_Spectra\_Mosq\_Guiana\_Body-parts\_IRS\_August-2023”.

551

552

553

554

555

556

557

558

559

560

561

562

563

564

565

566

567

568

569

570

571

572

573

574

575

576

577

578

579

580

581

582

583

584

585

586

587

588

589

590

591

592

593

594

595

596

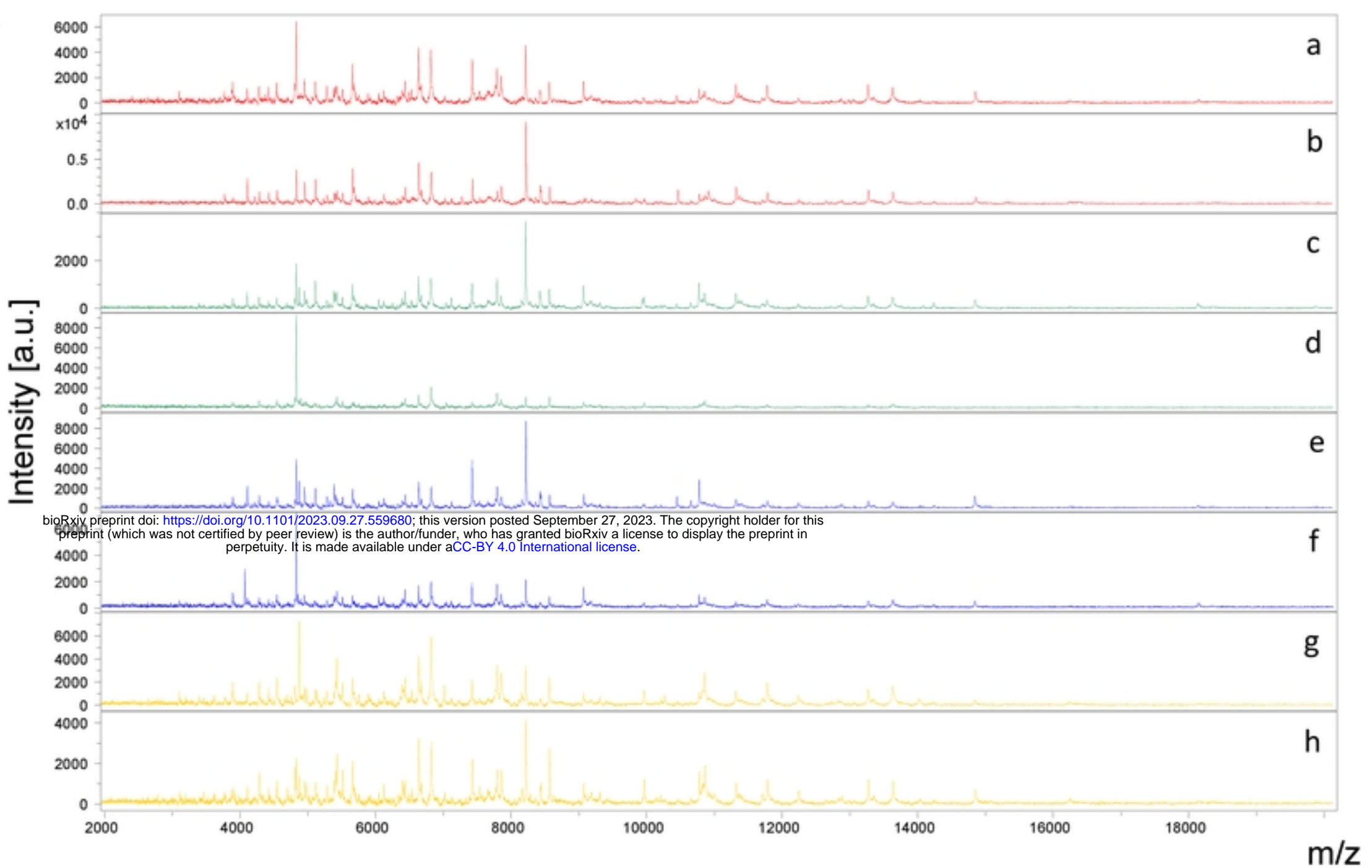
**Table S1.** Primer pairs used for detection of *kdr* mutation points.

| Primer name | Sequences            | PCR product (bp) | Mutation points analyzed |
|-------------|----------------------|------------------|--------------------------|
| 410F        | TTACGATCAGCTGGACCGTG | 150              | V410L (GTA/TTA)          |
| 410R        | TTACGATCAGCTGGACCGTG |                  |                          |
| 1016F       | ACAATGTGGATCGCTTCCC  | 612              | V1016I (GTA/ATA)         |
| 1016R       | GCAATCTGGCTTGTAACTTG |                  |                          |
| 1534F       | TCGCAGGAGGTAAGTTATTG | 350              | F1534C (TTC/TGC)         |
| 1534R       | GTTGATGTGCGATGGAAATG |                  |                          |

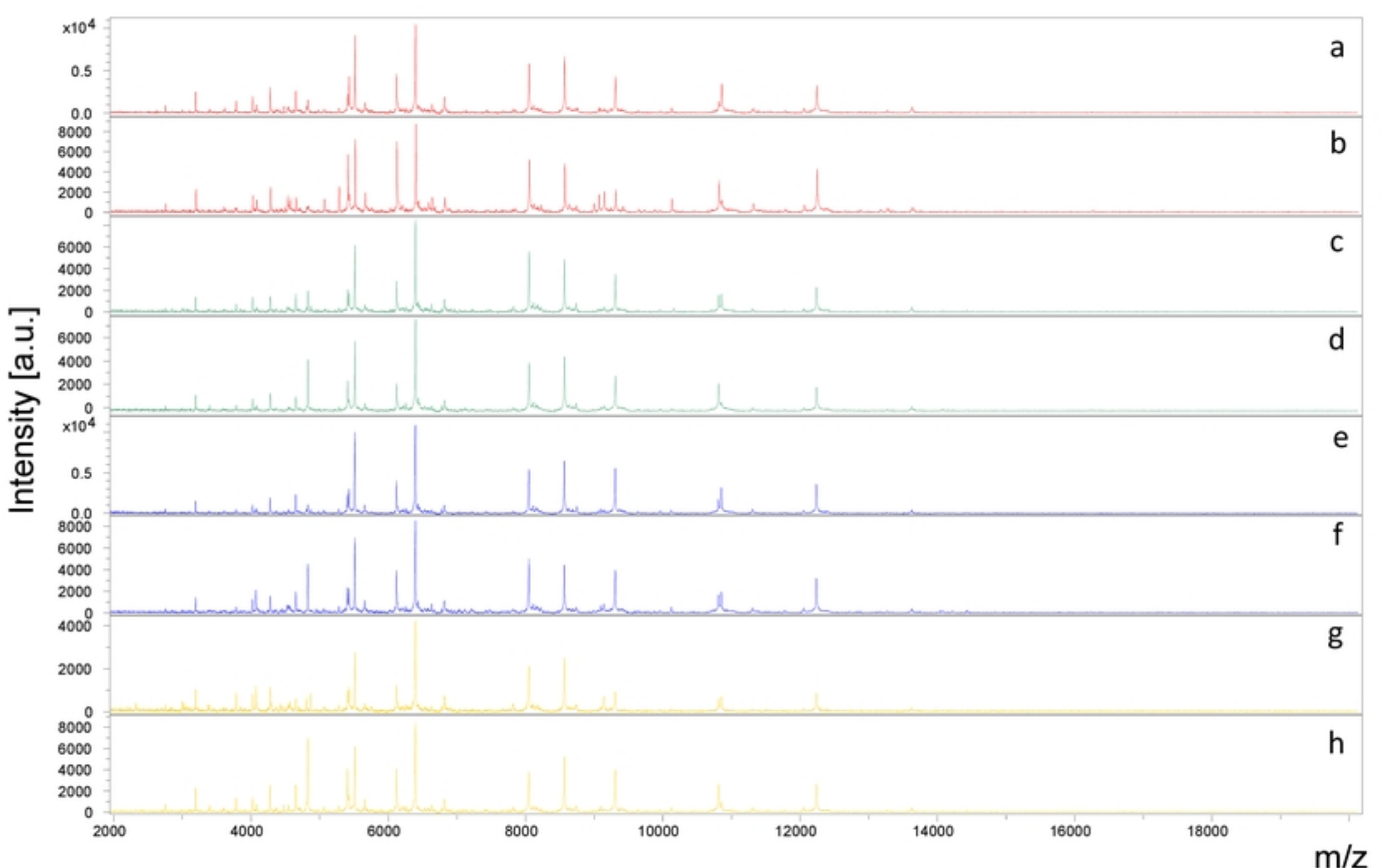
597 F, forward; R, reverse.

598

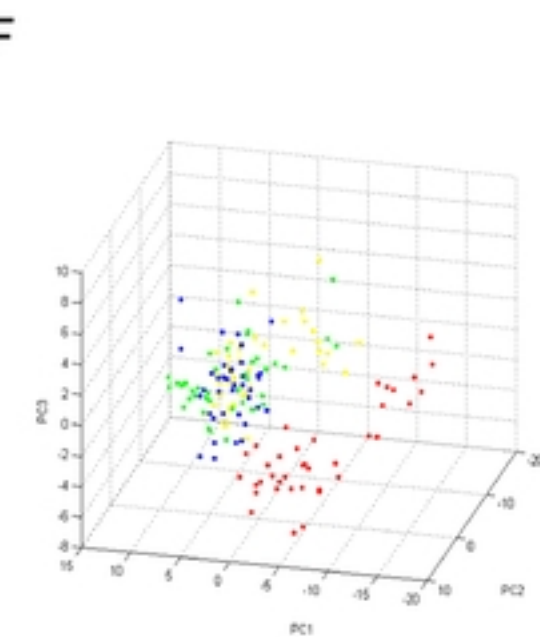
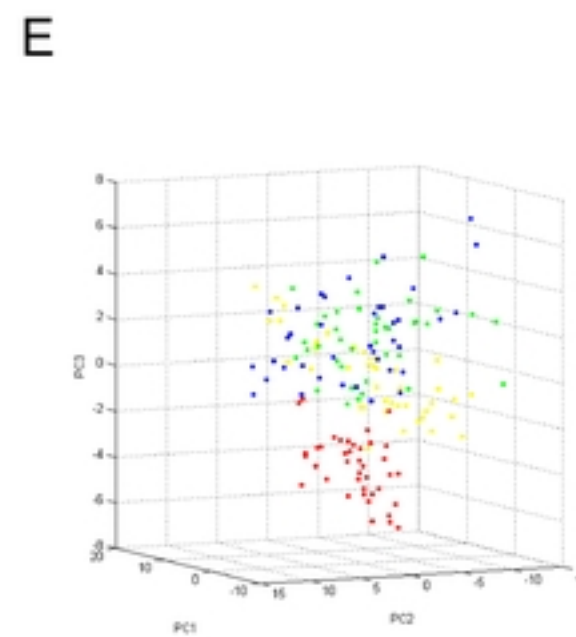
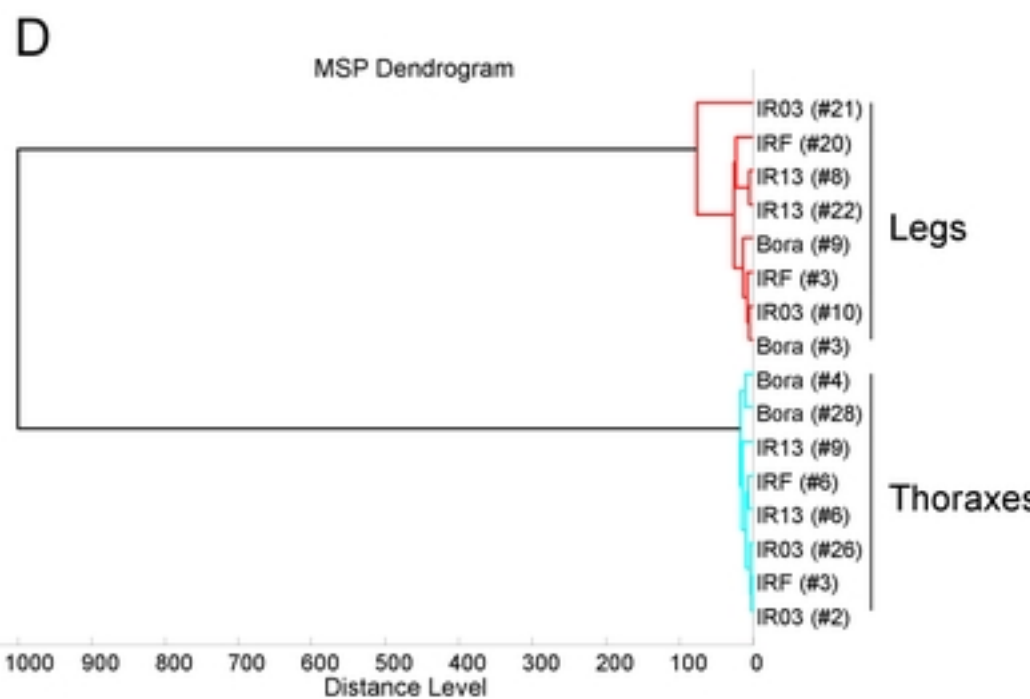
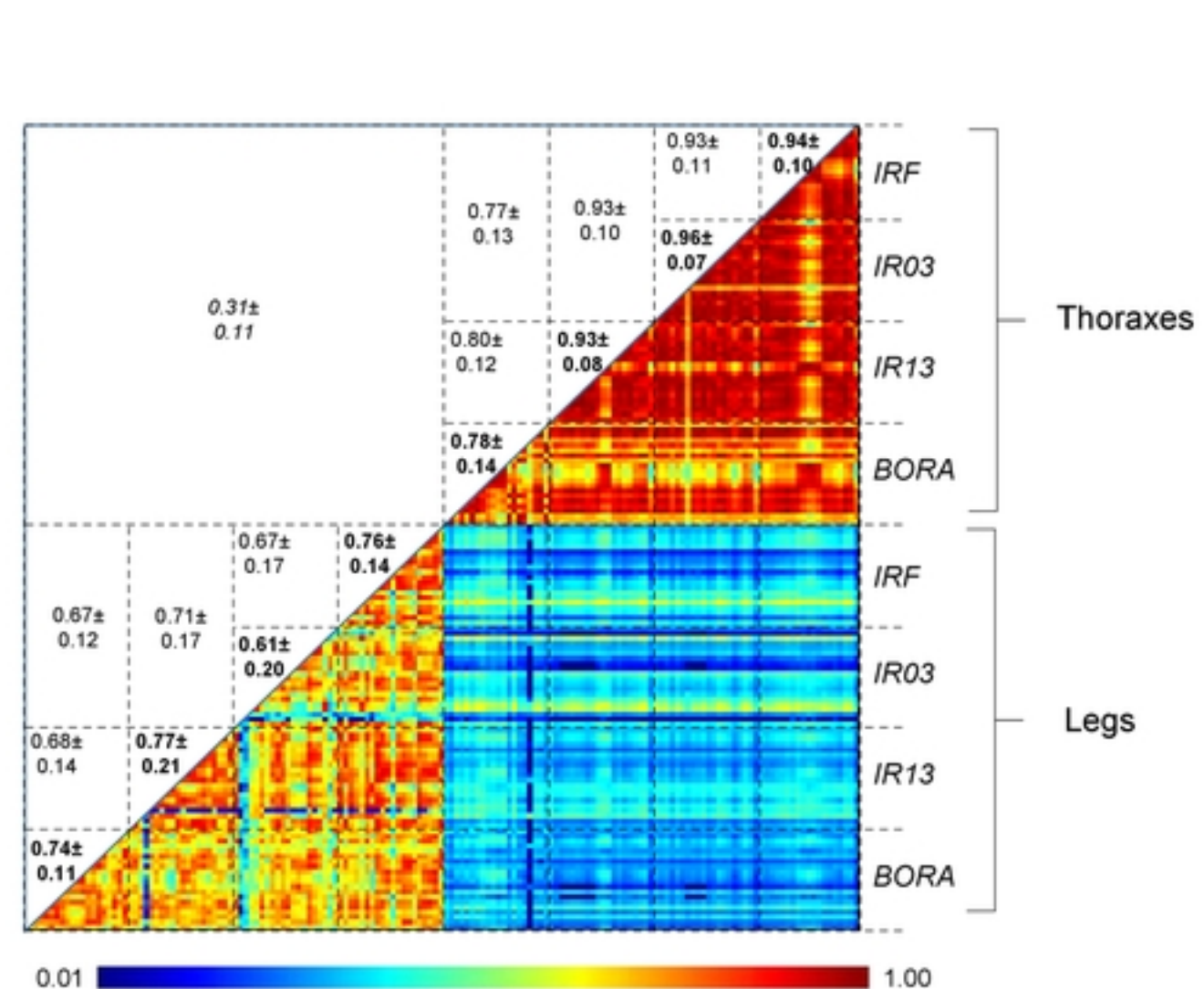
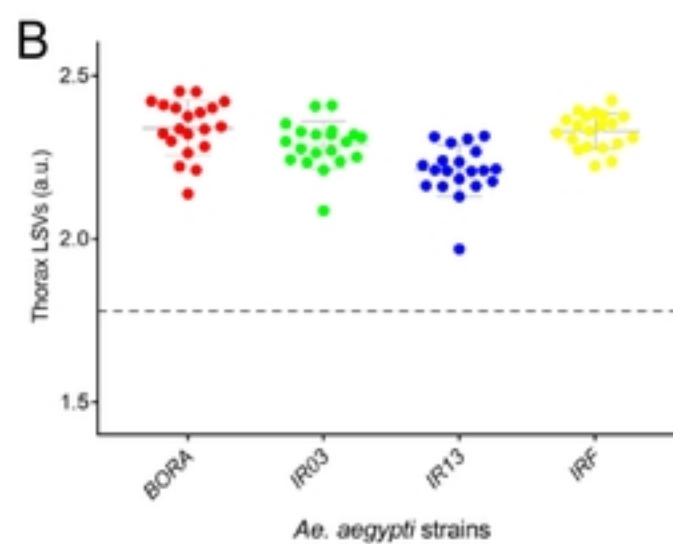
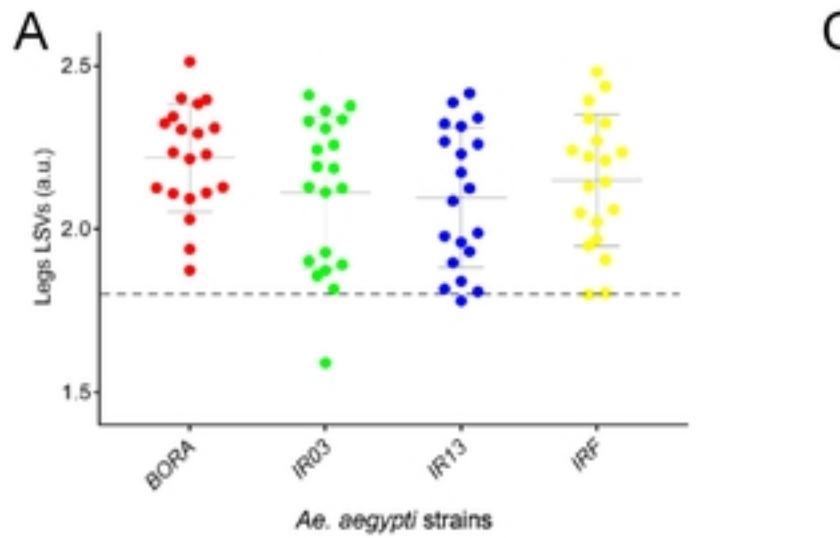
A



B

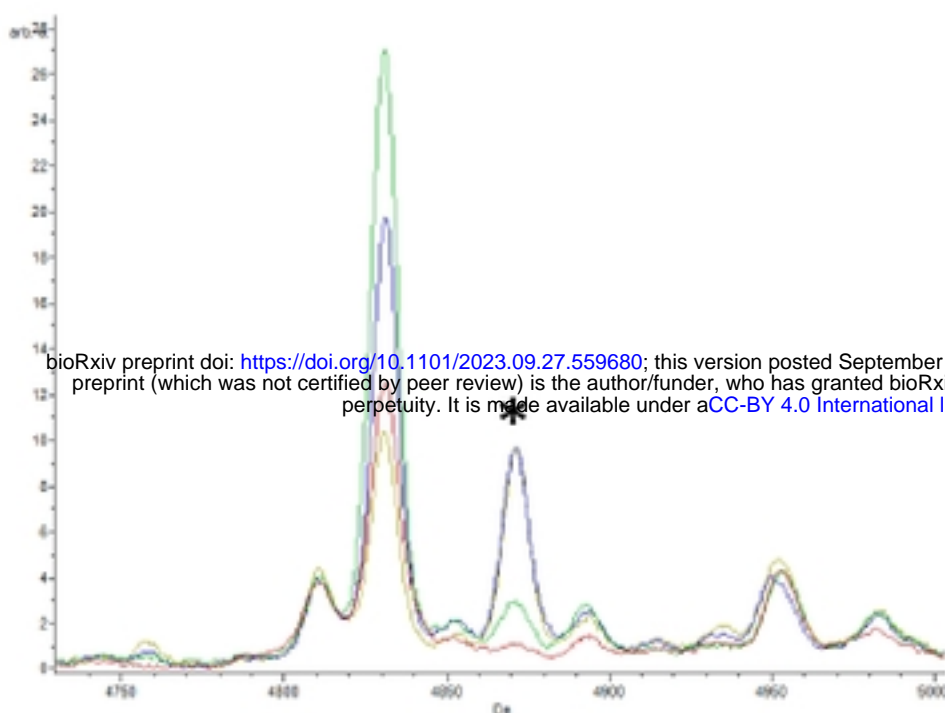


Figure\_1

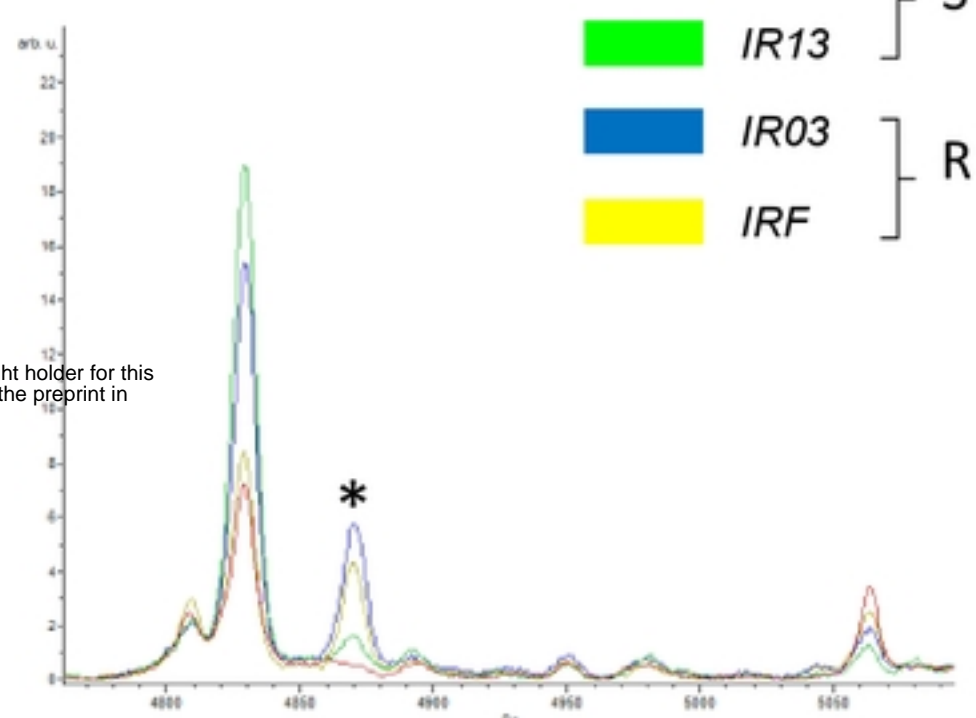


Figure\_2

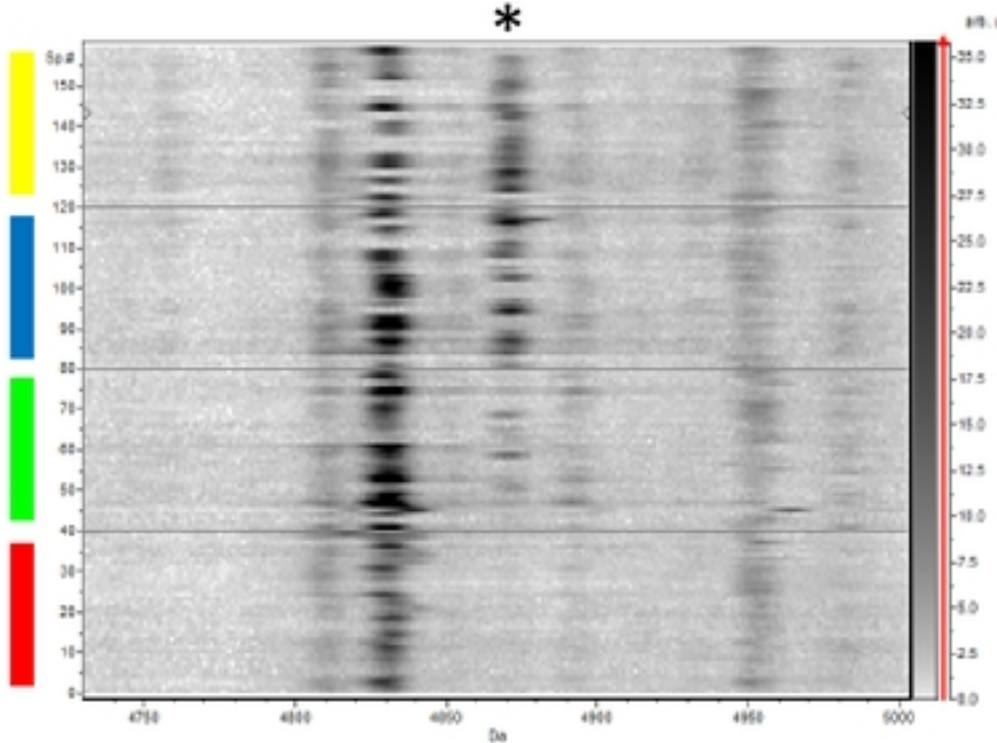
A



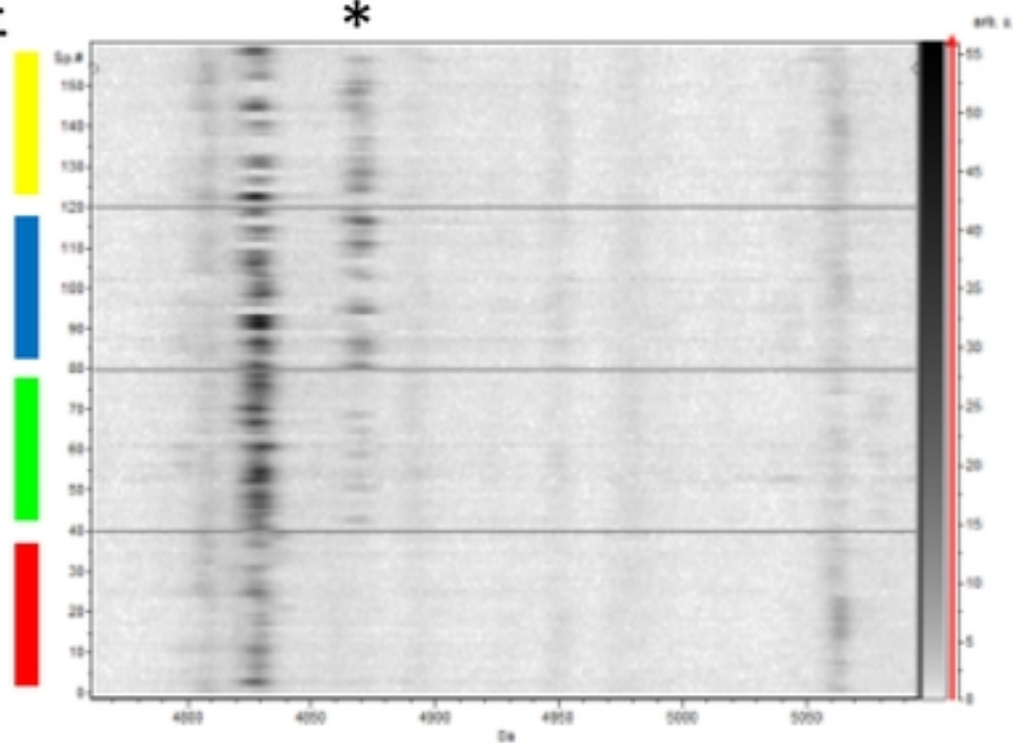
D



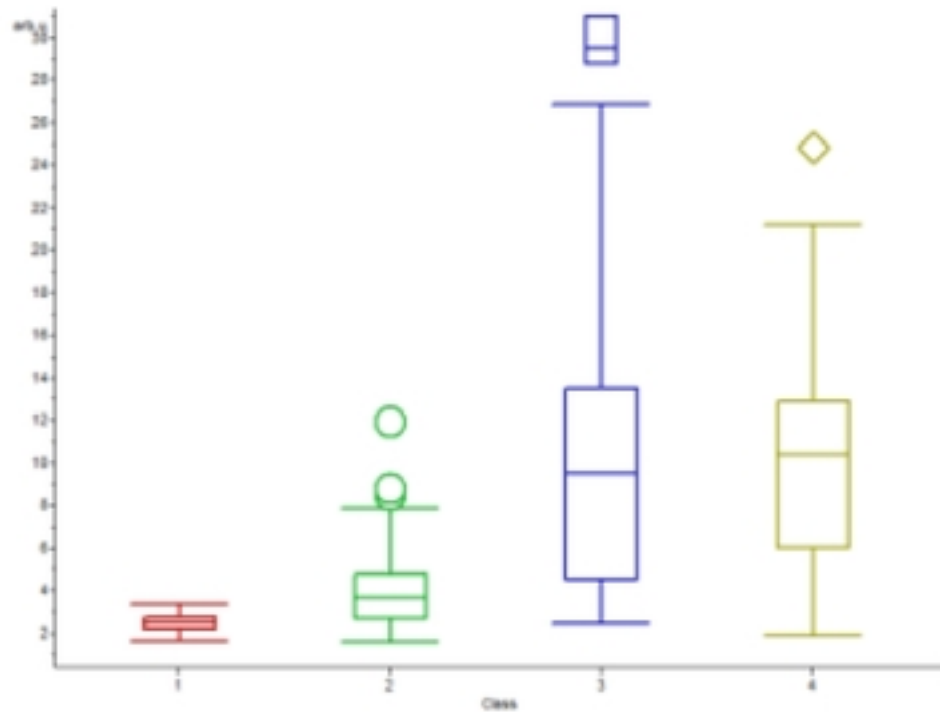
B



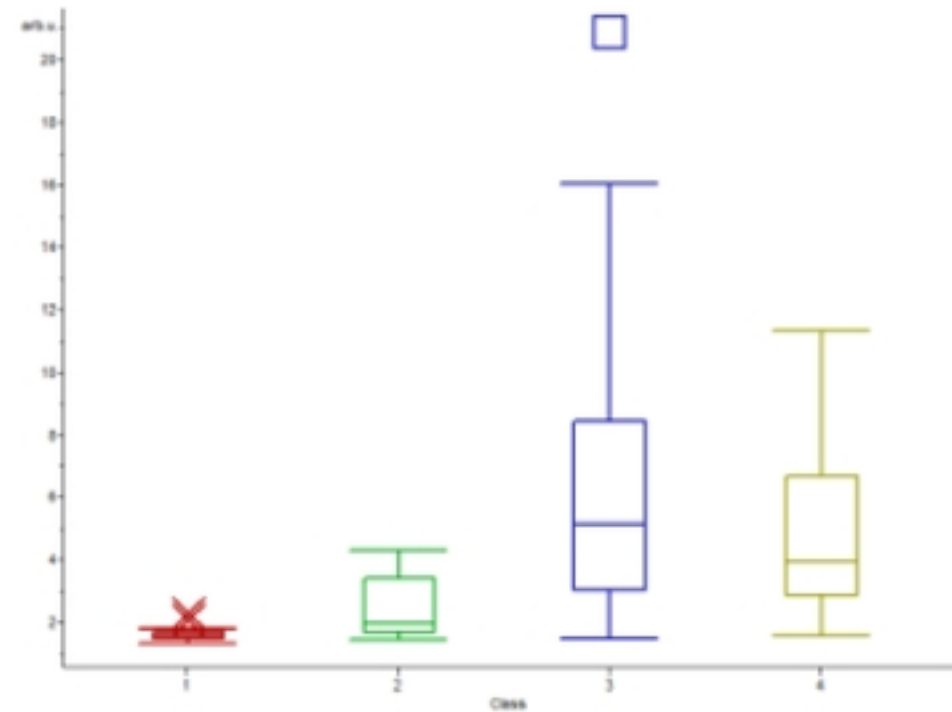
E



C



F



Figure\_3